Demand Side Management in Power Grid Enterprise Control: A Comparison of Industrial & Social Welfare Approaches

Bo Jiang, Aramazd Muzhikyan, Amro M. Farid, Kamal Youcef-Toumi

Abstract

Despite the recognized importance of demand side management (DSM) for mitigating the impact of variable energy resources and reducing the system costs, the academic and industrial literature have taken divergent approaches to DSM implementation. The prequel to this paper has demonstrated that the netload baseline inflation – a feature particular to the industrial DSM unit commitment formulation – leads to higher and costlier day-ahead scheduling compared to the academic social welfare method. This paper now expands this analysis from a single optimization problem to the full power grid enterprise control with its multiple control layers at their associated time scales. These include unit commitment, economic dispatch and regulation services. It compares the two DSM formulations and quantifies the technical and economic impacts of industrial baseline errors in the day-ahead and real-time markets. The paper concludes that the presence of baseline errors – present only in the industrial model – leads to a cascade of additional system imbalances and costs as compared to the social welfare model. A baseline error introduced in the unit commitment problem will increase costs not just in the day-ahead market, but will also introduce a greater netload error residual in the real-time market causing additional cost and imbalances. These imbalances if left unmitigated degrade system reliability or otherwise require costly regulating reserves to achieve the same performance. An additional baseline error introduced in the economic dispatch further compounds this cascading effect with additional costs in the real-time market, amplified downstream imbalances, and further regulation capacity for its mitigation.

NOMENCLATURE

Sets

b	index of buses
DC	subscript for dispatchable demand units (i.e. participating in DSM)
DS	subscript for stochastic demand units (i.e. conventional load)
GC	subscript for dispatchable generators (e.g. thermal plants)
GS	subscript for stochastic generators (e.g. wind, solar photo-voltaic)
h	index of lines
i	index of dispatchable generators
j	index of dispatchable demand units
k	index of stochastic generators
l	index of stochastic demand unit
t	index of time

Parameters

γ_{bt}	incremental transmission loss factor of bus b at time t

Bo Jiang is with the Mechanical Engineering Department at the Massachusetts Institute of Technology, Cambridge, MA, USA. bojiang@mit.edu

Aramazd Muzhikyan is with the Engineering Systems and Management at the Masdar Institute of Science & Technology, Abu Dhabi, UAE. amuzhikyan@masdar.ac.ae

Amro M. Farid is an Associate Professor of Engineering with the Thayer School of Engineering at Dartmouth, Hanover, NH, USA. He is also a Research Affiliate with the MIT Mechanical Engineering Department. amfarid@dartmouth.edu, amfarid@mit.edu

Kamal Youcef-Toumi is a Professor of Mechanical Engineering at the Massachusetts Institute of Technology, Cambridge, MA, USA. youcef@mit.edu

a_{bht} bus b generation shift distribution factor to line h at time t
A_{DCj} quadratic utility function coefficients of the j^{th} dispatchable demand unit
$\mathbb{A}_{DCj}$ quadratic cost function coefficient j^{th} virtual generation
A_{GCi} quadratic cost function coefficient of the i^{th} dispatchable generator
B_{DCj} linear utility function coefficients of the j^{th} dispatchable demand unit
$\mathbb{B}_{DCj}$ linear cost function coefficient j^{th} virtual generation
B_{GCi} linear cost function coefficient of the i^{th} dispatchable generator
$\Delta\hat{D}_{bt}$ stochastic demand forecast increments on bus b at time t
$\overline{F_h}$ flow limit of line h
M_{bi} correspondence matrix of dispatchable generator i to bus b
M_{bj} correspondence matrix of dispatchable demand unit j to bus b
N_B Number of buses
N_{DC} Number of dispatchable demand units
N_{GC} Number of dispatchable generators
$\underline{P_{DCj}}$ min. capacity of the j^{th} dispatchable demand unit
$\overline{P_{DCji}}$ max. capacity of the j^{th} dispatchable demand unit
$\underline{\tilde{P}_{DCj} - P_{DCj}}$ min. capacity of the j^{th} virtual generator
$\overline{\tilde{P}_{DCj} - P_{DCj}}$ max. capacity of the j^{th} virtual generator
$\underline{P_{GCi}}$ min. capacity of the i^{th} dispatchable generator
$\overline{P_{GCi}}$ max. capacity of the i^{th} dispatchable generator
$\underline{R_{DCj}}$ min. ramping capability of the j^{th} dispatchable demand unit
$\overline{R_{DCj}}$ max. ramping capability of the j^{th} dispatchable demand unit
$\underline{R_{GCi}}$ min. ramping capability of the i^{th} dispatchable generator
$\overline{R_{GCi}}$ max. ramping capability of the i^{th} dispatchable generator
T_{ED} real-time market time step

Decision Variables

$\Delta\mathcal{C}_{DCjt}$ incremental cost of the j^{th} virtual generator at time t
$\Delta\mathcal{C}_{GCit}$ incremental cost of the i^{th} dispatchable generator at time t
ΔD_{bt} dispatchable demand increments on bus b at time t
F_{ht} power flow level of line h at time t
ΔP_{DCjt} incremental power consumption at the j^{th} dispatchable demand unit in the t^{th} time interval
ΔP_{GCit} incremental power generation at the i^{th} dispachable generator in the t^{th} time interval
ΔP_{bt} dispatchable generation increments on bus b at time t
P_{DCjt} dispatched power consumption at the j^{th} dispatchable demand unit in the t^{th} time interval
$\tilde{P}_{DCjt} - P_{DCjt}$ dispatched power generation at the j^{th} virtual generator at time t
P_{GCit} dispatched power generation at the i^{th} dispachable generator in the t^{th} time interval
$\Delta\mathcal{U}_{DCjt}$ incremental utility of the j^{th} dispatchable demand unit at time t
$\Delta\mathcal{W}_t$ incremental social welfare at time t

I. Introduction

A. Motivation

The prequel [1] to this paper explains that the industrial and academic literature are taking divergent approaches to DSM implementation. DSM with its ability to allow customers to adjust electricity consumption in response to market signals provides additional dispatchable resources to mitigate the variable effects of renewable energy [2], [3], enhance electrical grid reliability and reduce system costs through load shaping and emergency response [4]–[9]. Research on DSM has studied the promotion effect of demand response on distributed generation [10], characterized the load shaping behavior of responsive demands in commercial, residential, and water sectors [11]–[14], and developed algorithms [15], [16] to achieve several optimization goals including minimizing customer discomfort and energy consumption [17], [18]. Recent studies have also addressed the effect of DSM energy & reserve market integration on reliability [19], the incorporation of storage and demand response in optimal power

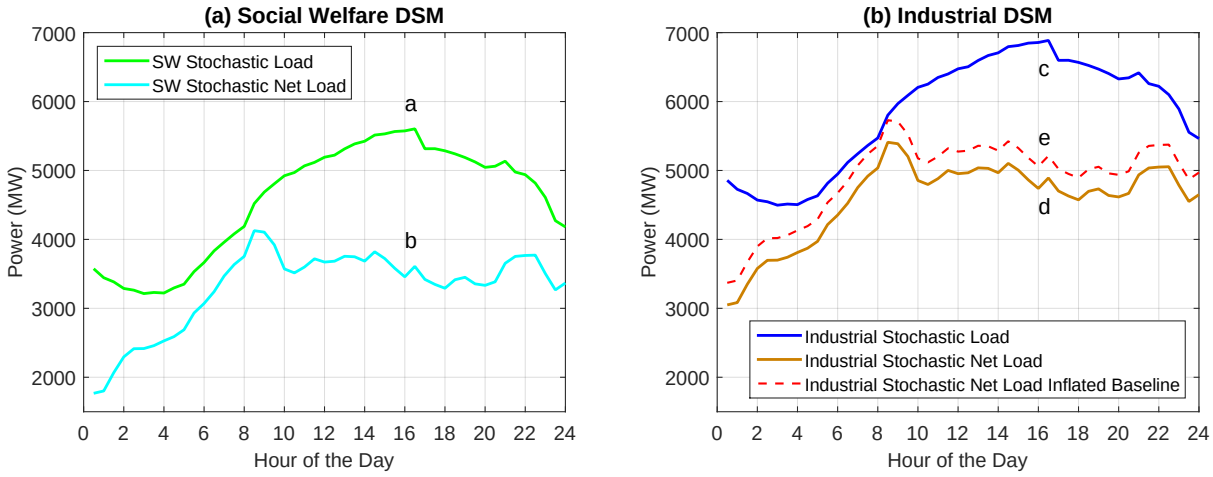

Fig. 1. Stochastic Net Load in SW and Industrial DSM

flow and energy hub design [20], [21], the scheduling of demand side storage, [22]–[24], and the integration of bus communication [25] and multi-agent systems [26] into DSM.

The demand response market design mostly commonly used among academic researchers [27]–[35] maximizes social welfare (SW); defined as the benefits from electricity consumption measured as a monetized utility minus the costs of generation [27]. The industrial trend, best exemplified by FERC order 745 [36]–[38], in contrast, minimizes the costs of generation and the compensation to customers for load reductions from a predefined electricity consumption baseline. Such a baseline is administratively set as the electricity consumption that would have occurred without DSM and is estimated from historical data after enrollment in the DSM program [39], [40]. In this way, dispatchable demand reductions are treated as "virtual generators". For the sake of brevity, these two market designs will be called the social welfare and industrial DSM models respectively.

The prequel [1] to this paper emphasized the need to rigorously compare these DSM market designs on an even footing despite their fundamental differences. Figure 1 contrasts stochastic load and net load curves in the two DSM implementations. In Figure 1(a), curve **a** represents the stochastic load in the SW model. It consists of the demand forecast from all non-DSM-participating customers. Subtracting the stochastic generation (e.g. wind & solar PV generation) from curve **a** gives curve **b**; representing the stochastic net load in the SW model. Note that this net forecasted time series is composed of two terms, does not include a baseline, and sets the aggregate values to which the controllable generation and demand must dispatch. In Figure 1(b), curve **c** represents the stochastic net load in the industrial model. It is the sum of curve **a** and the baseline estimation of customers participating in the industrial DSM program. Subtracting stochastic generation from curve **c** results in curve **d**; representing the stochastic net load in the industrial model. Note that this net forecasted time series is composed of three terms, one of which includes the industrial DSM baseline, and sets the aggregate values to which the controllable generation and "virtual" generation must dispatch. In other words, the industrial stochastic net load curve **d** is obtained by adding the industrial DSM baseline to the SW net load curve **b**. In the (likely) event [41], [42] that the industrial DSM baseline is erroneously inflated, an error term is added to curve **d** to become curve **e**; the effective net load curve to which energy resources are dispatched.

The topic of baseline inflation and its associated concerns have been raised in the literature [41], [42]. Previous studies have incorporated a baseline in several incentive and priced-based DSM programs [43] in different timescales [44]. The main concern around industrial DSM baselines is that customers have an implicit incentive to surreptitiously inflate it for greater compensation; taking advantage of their greater awareness of their own facilities relative to the regulatory agencies charged with estimating the baseline [41], [42], [45]. Despite this concern, a rigorous comparison of the two DSM market designs with and without demand baseline was only first conducted in [46], [47]. The prequel to this paper proved the equivalence of the two DSM models when implemented in a day-ahead market provided that 1) the utility function of dispatchable demand and the cost function of virtual generation are properly reconciled, 2) startup and shutdown costs are neglected and 3) the industrial DSM baseline is equivalent to the load forecast of the virtual generators had they opted out of the industrial DSM program [1].

This last condition of an accurate baseline forecast is likely unachievable, because load forecasts are calculated a day in advance based upon sophisticated methods [48], while the baseline calculation involves much more basic formulae determined months in advance [49]–[51]. Successful baseline manipulation has been shown to result in higher day-ahead dispatchable resources scheduling and higher costs in the unit commitment problem [1]. As a result, this baseline error has to be corrected in downstream enterprise control activities at faster time scales, likely requiring greater control efforts and greater operating reserve capacities and their associated costs [1], [52].

B. Contribution

As discussed above, the prequel to this paper [1] compares the day-ahead dispatches and operation costs of the system when social welfare and industrial DSM models are integrated into the day-ahead market structure. This limits the scope of the study to a single timescale of power system operations, namely the day-ahead market. In contrast, the goal of this paper is to compare the power system day-ahead and real-time operations when the two DSM designs are integrated into multiple timescales. In all, this paper extends the findings of the prequel [1] with the following three contributions. First, the power system operations are modeled as an enterprise control consisting of three control layers of the power system balancing operations on top of the physical power grid. The power system enterprise control was introduced in [53], [54] and is briefly described in Section II-A. The three control layers are the resource scheduling, implemented as a security-constrained unit commitment (SCUC), the balancing operations, implemented as a security-constrained economic dispatch (SCED), and the regulation service, implemented as an automatic generation control (AGC). The DSM models are incorporated into both day-ahead (SCUC) and real-time (SCED) market structures. Compared to the prequel [1], the integration of multiple control layers into a single simulator captures the coupling between different timescales and reveals the cross-timescale impacts of the DSM implementation. Second, this study compares the impacts of the social welfare and industrial DSM designs on the day-ahead and real-time operations. Utilization of the multi-layer enterprise control simulator also allows tracking cross-timescale impacts. Third, the implementation of the industrial DSM has a potential to introduce baseline errors into both SCUC and SCED formulations. This paper studies the impact of the SCUC and SCED baseline errors on the power system day-ahead and real-time operations. Both technical and economic aspects are addressed, namely the impact of the baseline errors on the power system operating reserve requirements, operation costs and the market prices. Here again, utilization of the enterprise control simulator helps to reveal cross-timescale impacts of the baseline errors.

C. Paper Outline

The remainder of this paper develops in five sections. Section II highlights important aspects of the literature on power grid enterprise control and demand side management. Section III develops two power grid enterprise control models with social welfare and industrial DSM designs respectively. Section IV describes the simulation scenarios and the simulation setup. Section V presents the simulation results and their discussion. Section VI makes recommendations on DSM implementation. The paper concludes in Section VII.

II. Background

This section describes the power grid enterprise control model in terms of control layers, variable energy characterization, and types of reserves. It also summarizes the highlights from the social welfare and industrial DSM models.

A. Enterprise Control

The enterprise control assessment method for variable energy resource induced power system imbalances has been recently developed to reflect typical balancing operations in American ISOs [53]–[55]. It uses a simulation package which consists of three integrated control layers and the physical power grid: resource scheduling layer, balancing actions layer, and a regulation service layer. Prior to this development, extensive academic and industrial works have studied each of the layers individually neglecting the coupling between layers [56]–[66]. A recent review on variable energy resource integration concludes that the literature has several significant methodological limitations [59]. Existing studies are case specific [67], only address a single control function of power grid balancing operations

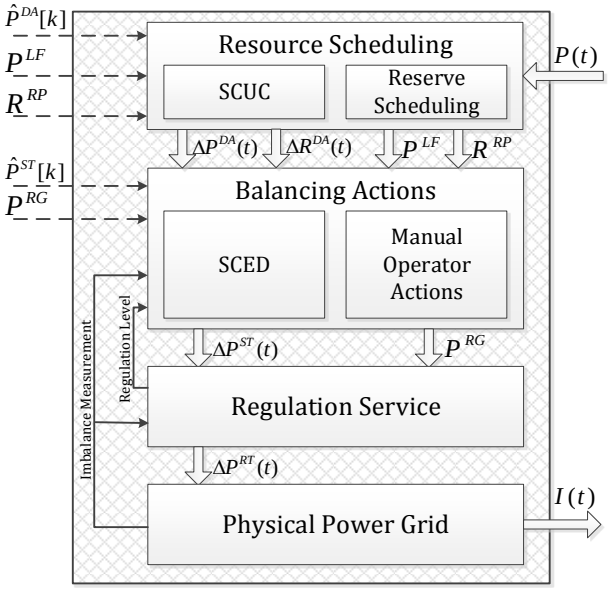

Fig. 2. Architecture Model of a Power Grid Enterprise Control Simulator [53]

at a specific time scale [68], or are limited to statistical calculations [69]. The recent publications on power grid enterprise control distinguish themselves in that they are specifically developed to reflect the holistic balancing performance of a modern American ISO [53], [54]. In contrast to many traditional academic works, this holistic assessment method is case-independent, addresses both the physical grid as well as enterprise control processes, and is validated by a set of numerical simulations.

The power system enterprise model encompasses three consecutive control layers on top of the physical grid: resource scheduling layer in the form of a security-constrained unit commitment (SCUC), balancing actions in the form of a security-constrained economic dispatch (SCED) and manual actions, and a regulation service in the form of automatic generation control (AGC) [53]. Each lower layer operates at a smaller timescale resulting in subsequently smaller imbalances. The SCUC uses the day-ahead netload forecast to schedule generation with a coarse time resolution. The SCED uses the available load following and ramping reserves to re-dispatch generation units in the real-time market using the short-term netload forecast. Figure 2 shows a graphical illustration of the enterprise control model. The following notations are used in the graph.

$P(t)$	Stochastic net load	$\hat{P}_{ST}(t)$	Stochastic net load short-term forecast
$\hat{P}_{DA}(t)$	Stochastic net load day-ahead forecast	P_{REG}^{REQ}	Regulation reserve requirement
P_{LOAD}^{REQ}	Load following reserve requirement	$\Delta P_{ST}(t)$	Residual imbalances at SCED output
R_{RAMP}^{REQ}	Ramping reserve requirement	P_{REG}	Scheduled regulation reserves
$\Delta P_{DA}(t)$	Residual imbalances at SCUC output	$\Delta P_{RT}(t)$	Residual imbalances at regulation output
P_{LOAD}	Scheduled load following reserves	$I(t)$	System imbalances
R_{RAMP}	Scheduled ramping reserves		

The regulation service layer modeling is inherited from [53], where the available regulation reserves are used to fine-tune the system balance. The regulation service is provided by generation units with AGC (feedback loop) capabilities [70]. In implementation, the regulation service responds to the imbalance by moving its output to the opposite direction until the imbalance is mitigated or generators are saturated. For steady-state simulation, a designated virtual slack generator consumes the mismatch of generation and consumption to make the steady-state power flow equations solvable [53], [71].

The consideration of multiple layers of enterprise control has facilitated methodological improvements in the determination of operating reserve requirements. Rather than case-specific heuristics, several new analytical derivations of operating reserve requirements have recently been advanced in the literature [72]–[75]. They are presented as functions of variable energy resources (VER) characteristics including penetration level, VER capacity factor, variability, and forecast errors [72]–[75]. The penetration level is the VER capacity normalized by the system peak load, the capacity factor is the average VER power output per installed capacity; and the penetration level and capacity factor together determine the actual VER output. Variability is a measure of the rate of change VERs. The VER forecast error adopts the standard deviation of the difference between the best and actual VER forecasts normalized by the installed capacity [53]. The day-ahead forecast error is used by the SCUC problem, while the short-term forecast error is an input to the SCED problem. Readers are referred to [53] for detailed description of each control layer and the formal definitions of the five VER parameters listed above. References [53], [69], [76] include the definitions of reserve types, namely load following and ramping reserves used in the real-time market, and the regulation reserves used in the regulation service.

B. Social Welfare vs Industrial DSM

The simplest form of the social welfare maximization found in [27] is commonly used in academic research. It consists of an elastic demand characterized by its utility or benefits from electrical consumption. It also includes the cost of generation [27]. The optimization determines the electricity prices and setpoints for all dispatchable resources simultaneously to maximize the net benefits [33].

Much like the social welfare model, the industrial DSM dispatch schedule and price are jointly determined by suppliers and consumers [33] to minimize the total cost of the dispatchable and (demand-side) virtual generators. A curtailment service provider (CSP) represents the demand unit participating in the wholesale energy market. Each CSP has an "administratively-set" electricity consumption baseline as an estimate of consumption without DSM incentives and from which load reductions are measured. The CSP can participate in one or more wholesale energy markets [77], where generation suppliers, load serving entities, and CSPs bid through an ISO/RTO [78]. The bidding process determines the dispatched resources as well as the electricity price [38]. Accepted load reductions are subsidized by ISO/RTO based on the bidding price compared to the Locational Marginal Pricing (LMP) and the Retail Rates (GT) [79]. DSM participating customers have an implicit incentive to surreptitiously inflate the administrative baseline for greater compensations. For example, the customers can artificially increase their electricity consumption when baselines are being evaluated [41]. Customers who anticipate to reduce loads regardless of DSM are also more likely to be attracted to participate [41]. Successful baseline manipulation may cause generation relocation and inefficient price information [41].

III. Model Development: Power Grid Enterprise Control with Demand Side Management

As mentioned in Section I-B, this paper provides a rigorous comparison of the techno-economic performance of the social welfare and industrial DSM implementations. To that end, the power grid enterprise control simulator described in Section II-A is used as an assessment tool. One important feature of the simulator is its modular architecture (shown in Figure 2) which allows for each of its modules to be modified in its functionality. This has facilitated the study of renewable energy [53], [54] and energy storage resource [52], [55] integration. The interested reader is referred to [53], [54] for a detailed description of its three layers of enterprise control which rest upon a model of the physical power grid.

In order to study the techno-economic performance of the social welfare and industrial DSM implementations, the SCUC and SCED modules in Figure II-A have been modified. The social welfare and industrial DSM implementations for the SCUC problem have been presented in detail previously [1]. The remainder of the second presents the social welfare and industrial DSM implementations for the SCED problem. The two models are then reconciled.

A. Social Welfare SCED Model

The social welfare SCUC optimization program with dispatchable demands has been described in detail in the prequel to this paper [1]. The optimization goal is to achieve maximum social welfare defined as the net benefit from electricity consumption and generation over all time intervals subject to power balance constraint. Both the

utility from dispatchable demand and cost from dispatchable generation have a start-up, a shut-down, and a running component. All running utility and generation cost functions are modeled as second-order functions with respect to power levels.In addition, all dispatchable generation and dispatchable demand units are subject to their respect maximum and minimum capacity limits, maximum and minimum ramping limits, as well as the logical constraints where the on or off states need to be consistent with the start-up and shut-down states.

In the subsequent real-time market, the SCED moves the available dispatchable generation and demand units to new setpoints based on the short-term netload forecast. In contrast to the SCUC, the linearized SCED problem runs at each real-time dispatch time point and determines the incremental power for one time step, and it only dispatches units determined online by SCUC. The SCED utilizes the on/off decision from SCUC dispatch instead of making state decisions. Transmission analysis is included. Some input parameters depend on the current state of the system, and are calculated prior to each SCED iteration based on a full AC power flow analysis of the system [53]. The optimization goal is to maximize incremental social welfare, formulated as the first derivative of the social welfare function:

$$\Delta \mathcal{W}_t = \sum_{j=1}^{N_{DC}} \Delta \mathcal{U}_{DCjt} - \sum_{i=1}^{N_{GC}} \Delta \mathcal{C}_{GCit} \tag{1}$$

where

$$\Delta \mathcal{U}_{DCjt} = B_{DCj} \Delta P_{DCjt} + 2A_{DCj} P_{DCjt} \Delta P_{DCjt} \tag{2a}$$

$$\Delta \mathcal{C}_{GCit} = B_{GCi} \Delta P_{GCit} + 2A_{GCi} P_{GCit} \Delta P_{GCit} \tag{2b}$$

subject to power balance constraint in (3).

$$\sum_{l=1}^{N_B} (1 - \gamma_{bt})(\Delta P_{bt} - \Delta D_{bt} - \Delta \hat{D}_{bt}) = I_t + G_t \tag{3}$$

where I_t is the current level of imbalances, G_t is the current level of utilized regulation reserves, and:

$$\Delta P_{bt} = \sum_{i=1}^{N_{GC}} M_{bi} \Delta P_{GCit}, \quad \Delta D_{bt} = \sum_{j=1}^{N_{DC}} M_{bj} \Delta P_{DCjt} \tag{4}$$

The incremental transmission loss factor (ITLF) γ_{bt} for bus b shows how much the total system losses change when power injection on bus b increases by a unit [80]. Line flow limits are shown in (5). The generation shift distribution factor (GSDF) a_{hbt} shows how much the active power flow through line h changes when injection on bus b increases by a unit [80], [81]. Additional constraints include capacity limits on dispatchable demand and generation units in (6 & 7), and ramping limits on dispatchable demand and generation units in (8 & 9) respectively.

$$\sum_{l=1}^{N_B} a_{hbt} (\Delta P_{bt} - \Delta D_{bt} - \Delta \hat{D}_{bt}) \leq \overline{F_h} - F_{ht} \tag{5}$$

$$\underline{P_{DCj}} - P_{DCjt} \leq \Delta P_{DCjt} \leq \overline{P_{DCji}} - P_{DCjt} \tag{6}$$

$$\underline{P_{GCi}} - P_{GCit} \leq \Delta P_{GCit} \leq \overline{P_{GCi}} - P_{GCit} \tag{7}$$

$$\underline{R_{DCj}} * T_{ED} \leq \Delta P_{DCj} \leq \overline{R_{DCj}} * T_{ED} \tag{8}$$

$$\underline{R_{GCi}} * T_{ED} \leq \Delta P_{GCi} \leq \overline{R_{GCi}} * T_{ED} \tag{9}$$

The incorporation of ITLF into the model linearizes the power balance constraint; the incorporation of GDSF linearizes the line flow limit constraint (5).

B. Industrial SCED Model with Demand Baseline

The industrial SCUC optimization program integrating dispatchable demand has been described in detail in [1]. The optimization goal of the industrial approach is to minimize the total cost of dispatchable generators and virtual generators over all time intervals of the SCUC period, where the virtual generation cost is the compensation paid to a customer for reducing electricity consumption from the predefined demand baseline. In the industrial practice, the optimization aims to minimize total system costs including dispatchable and virtual generation costs. The cost functions of the dispatchable generation remain the same as in the social welfare model. The constraints on dispatchable generators remain the same as in the social welfare model, while the virtual generators are subject to maximum and minimum capacity limits, maximum and minimum ramping limits, as well as the logical constraints where the on or off state needs to be consistent with the start-up and shut-down state. The running cost is similarly modeled as a quadratic function of the load reduction from the baseline [1]. Like the SW model, the industrial SCED optimizes for one time step and includes transmission losses. The optimization goal is to minimize the total incremental cost, formulated as the first derivative of the cost function:

$$\sum_{i=1}^{N_{GC}} \Delta\mathcal{C}_{GCit} + \sum_{j=1}^{N_{DC}} \Delta\mathcal{C}_{DCjt} \tag{10}$$

where the dispatchable generation incremental costs formulation remains the same and

$$\Delta\mathcal{C}_{DCjt} = -\mathbb{B}_{DCj}\Delta P_{DCjt} - 2\mathbb{A}_{DCj}P_{DCjt}\Delta P_{DCjt} \tag{11}$$

The optimization is subject to the same power balance constraint in (3) and line flow limits in (5), capacity limits for virtual and dispatchable generation units in (12 & 7), and ramping limits for virtual and dispatchable generation units in (8 & 9) respectively.

$$(\tilde{P}_{DCjt} - P_{DCjt}) - \underline{\tilde{P}_{DCj} - P_{DCj}} \leq \Delta P_{DCjt} \tag{12a}$$

$$-\Delta P_{DCjt} \leq -\overline{\tilde{P}_{DCj} - P_{DCj}} - (\tilde{P}_{DCjt} - P_{DCjt}) \tag{12b}$$

C. Model Reconciliation

The two DSM methods are reconciled such that the loss in utility in the SW model is equal to the increase in virtual generation cost. The economics rationale is that the customers are only willing to cut down electricity consumption if their marginal loss in utility is subsidized by the marginal cost in virtual generation. The reconciliation leads to the following relations:

$$\mathbb{A}_j = -A_j, \quad \mathbb{B}_j = 2 * A_j * \tilde{P}_{DCj} + B_j \tag{13}$$

IV. Case Study

The main objective of this paper is to compare the social welfare and industrial DSM designs when integrated into multiple timescales of power system operations. Additionally, the industrial DSM has a potential to introduce baseline errors into both SCUC and SCED formulations, bringing uncertainties into the power system scheduling and balancing operations. Thus, this paper also studies the impact of such baseline errors on power system imbalances, operating reserve requirements and the operating costs. To that end, five scenarios are studied as described in the following subsection.

A. Simulation Scenarios

To study the impact of the baseline error on power system operations, the following five scenarios are simulated:

1) **System performance comparison for social welfare and industrial DSM models.** The differences in the social welfare and industrial DSM formulations define how the power system performance changes when each approach is implemented. The prequel to this paper [1] has studied the impact of SCUC baseline error on the generation levels and the operation cost of the day-ahead dispatch. This paper now uses the enterprise control model to study the impact of both SCUC and SCED baseline errors across different timescales. To that end,

the power system is simulated with 10% SCUC and SCED baseline errors, and the impact on the day-ahead and the real-time dispatches is studied.

2) **Impact of SCUC baseline error on power system imbalances and operating reserve requirements.** Presence of the baseline error introduces uncertainties into the system, which is shown to increase the potential imbalances [53], [54] and the reserve requirements [72]–[75]. However, since the reserves act at the timescales of their associated control layers, the impact of the SCUC baseline error on some of them may be significant, while negligible or absent on others.
3) **Impact of SCED baseline error on power system imbalances and operating reserve requirements.** The SCED baseline error, in contrast to the SCUC baseline error, occurs at a different timescale and, therefore, is expected to have larger impact on the corresponding reserve requirements. These two scenarios combined give the complete picture of how the baseline errors at different timescales bring new level of imbalances into the power system and require additional reserves to mitigate them.
4) **Impact of SCUC baseline error on power system operation cost and electricity market price.** As already mentioned above, the presence of SCUC baseline error alters the day-ahead dispatch of the system, which will inevitably impact the day-ahead scheduling cost and electricity market price. Additionally, incorporation of the enterprise control model into the simulations allows capturing any possible impact of the SCUC baseline error on the *real-time* operations. While the real-time market (SCED) operates at a different timescale, the impact of the SCUC baseline error can potentially propagate through the enterprise control layers and alter the real-time operations.
5) **Impact of SCED baseline error on power system operation cost and electricity market price.** The SCED baseline error occurs during the real-time operations and is expected to alter the real-time operation cost and electricity market price. However, similar to the previous scenario, any potential impact of the SCED baseline error on the day-ahead operations will also be studied. These two scenarios together establish the impact of the baseline errors on the economics of the power system operations.

Each simulation described above is run for one day of power system operations. The SCUC is implemented with 1-hour time resolution. The SCED and regulation service run over the course of the day and have time steps of 5 minutes and 1 minute respectively. The enterprise control simulator is implemented in MATLAB interfaced with GAMS. The SCUC is implemented as a mixed integer quadratic constraint (MIQCP) program in GAMS and solved using CPLEX. The rest of the simulator is implemented in MATLAB. A single day of simulation lasts approximately 196 seconds with an Intel(R) Core(TM) i7-4600 CPU at 2.10GHz on 8.00GB RAM, which is a 20% increase in time over the same optimization without dispatchable demand.

B. Simulation Setup

The scenarios are simulated using the enterprise control simulator implemented in accordance to Figure 2 [53], [54]. The physical power grid layer uses the IEEE RTS-96 (Reliability Test System-1996) configuration [82], consisting of 99 generators and 73 buses with $8550MW$ peak load. The generation cost data is taken from [83]. Since modeling and controlling each individual distributed dispatchable load would be unreasonable in actual operations and likely prevent timely and efficient dispatch decisions, this work assumes aggregated dispatchable demands are placed at each bus. However, a random distribution of dispatchable units on the buses may lead to heavy congestions on some transmission lines. Therefore, in the social welfare model, the minimum and maximum capacity limits of each dispatchable demand are set to zero and 30% of the peak load at the corresponding bus respectively. The SCUC and SCED baseline errors are represented as dimensionless units normalized to the dispatchable demand capacity on each bus. The utility function coefficients for all dispatchable demand units are assumed time-invariant. In the industrial model, an accurate baseline equals the maximum capacity of the dispatchable demand in the social welfare model. The cost functions of virtual generators are calculated from the reconciliation presented in Section III. The startup and shutdown costs of dispatchable demand units and virtual generators have entirely different physical meanings in the social welfare and industrial DSM models and are set to zero for fairness of the comparison.

The stochastic load in the social welfare represents the load from the non-participating customers. Load and wind daily profiles are taken from Bonneville Power Administration (BPA) repositories with 5 minutes resolution [84], [85]. The data is up-sampled to a 1-minute resolution [54] to match the needs of this study. Wind generation is

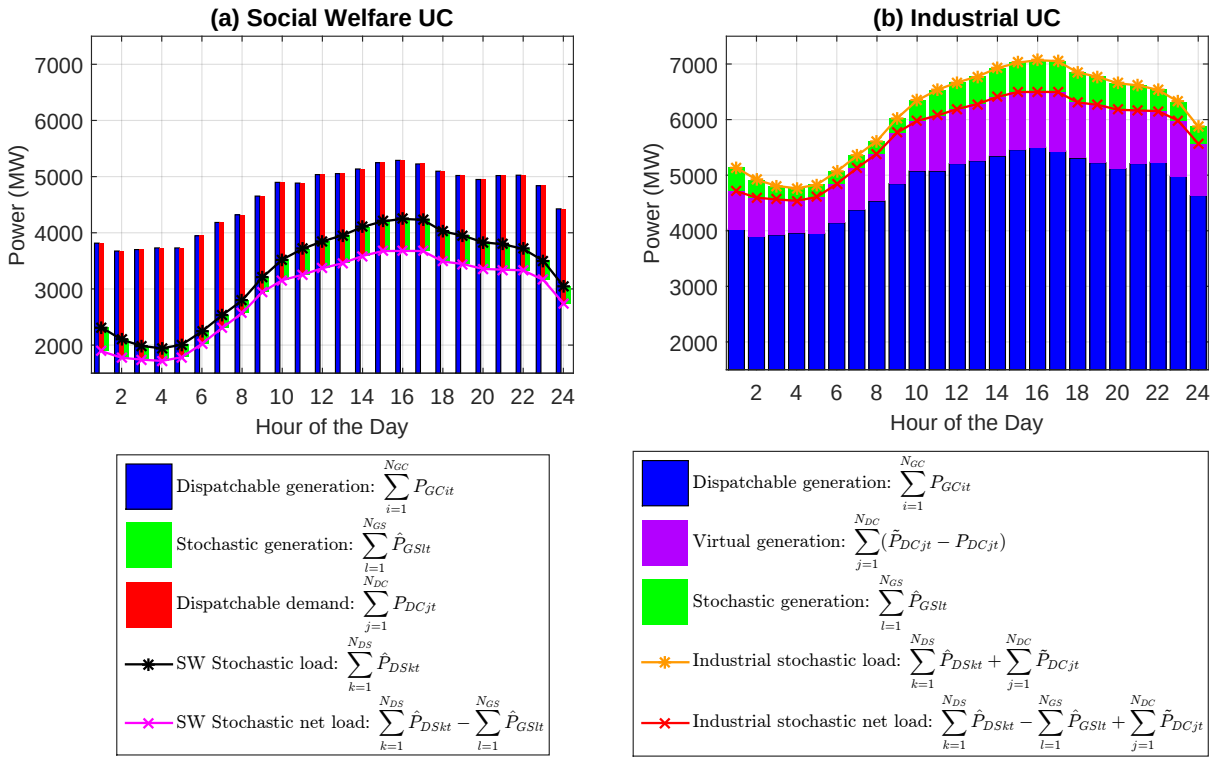

Fig. 3. Social Welfare vs. Industrial SCUC Dispatch – a.) includes dispatchable generation and demands to meet SW stochastic net load, b.) includes dispatchable and virtual generation to meet industrial stochastic net load

assumed to have 20% penetration level in accordance to the US renewable energy integration targets [86], [87] and current operations in some states [88]. The total wind generation is distributed on the system buses proportional to the peak loads on the corresponding buses in accordance to [53]. As a result, their profiles are perfectly correlated. Because the goal of this paper is to compare two enterprise control structures with different demand response implementations, this additional variable reflecting the cross-correlation is unnecessary. The impact of this cross-correlation on the power system operations can be subject of a different study. For the sake of simplicity, this study also assumes zero forecast errors for the stochastic load and wind, except for the first scenario. Since both the forecast error and the baseline error introduce uncertainties into the system and, therefore, have similar impacts, the presence of load and wind forecast errors would overpower the impact of the baseline error and make it harder to observe.

V. Simulation Results and Discussion

This section presents the simulation results and their discussion. Each subsection is devoted to one scenario.

A. System Performance Comparison for Social Welfare and Industrial DSM Models

This section compares the performances of the social welfare model and the industrial DSM model with 10% SCUC and SCED baseline errors. Figure 3 represents the results for the SCUC dispatch by both methods. As explained in Figure 1, the stochastic net load is different in the social welfare and industrial DSM model. The stochastic net load in the social welfare is composed of two terms, while in the industrial DSM model the stochastic net load is composed of three terms with an additional baseline estimation. Figure 3(a) shows the results for the social welfare model. The stochastic net load of the social welfare model (magenta line) is the difference between the stochastic demand (black line) and the wind generation (green bars). The dispatchable generation (blue bars) meets the sum of the stochastic net load and the dispatchable demand (red bars).

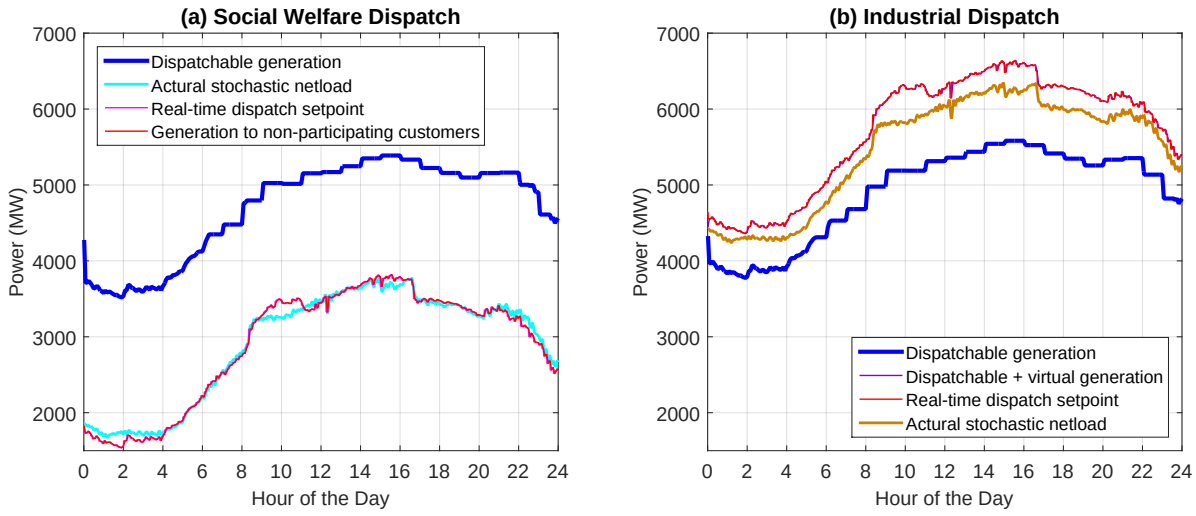

Fig. 4. Social Welfare vs. Industrial SCED Dispatch – a.) includes dispatchable generation and demands to meet SW Stochastic net load b.)includes dispatchable and virtual generation to meet industrial stochastic net load

Figure 3(b) shows the results for the industrial model with 10% SCUC and SCED baseline errors. The orange line shows industrial stochastic load including load from non-participating customers and the baseline load from DSM participants. The subtraction of the wind generation (green bars) gives the industrial stochastic net load (red line). It is met by the sum of dispatchable generation (blue bars) and virtual generation (purple bars). Comparing Figure 3(a) and 3(b) shows that the baseline inflation results in erroneously high dispatchable and virtual generation. The excess dispatchable generation will be offset in real-time by the SCED given the presence of enough load-following reserves. Otherwise, it will be further carried over to the regulation layer.

Figure 4 shows the SCED dispatch results, where Figure 4(a) uses the social welfare model and Figure 4(b) uses the industrial DSM model. The red line in Figure 4(a) represents the generation allocated to the stochastic load of non-participating customers. The magenta line, hidden behind the red line, represents the real-time dispatch setpoints that meet the red line every five minutes of the SCED dispatch. The dispatchable generation (blue line) is obtained by adding the dispatchable demand and the associated transmission losses on top of the red line. Lastly, the actual real-time net load is represented by the cyan line. The deviation between the setpoints and the actual net load is mainly due to the stochastic load and wind forecast errors.

Figure 4(b) shows the SCED dispatch results for the industrial model with 10% baseline errors. The red line represents the real-time dispatch setpoints. The stochastic net load of the industrial model exceeds that of the social welfare model by the baseline error. The blue line is the dispatchable generation. The purple line, hidden behind the red line, is the total generation equal to the sum of the dispatchable and virtual generations. The actual industrial stochastic net load is represented by the brown line. The large gap between the setpoints and the actual net load is mostly due to the baseline error, in addition to the stochastic load and wind forecast errors.

B. Impact of SCUC Baseline Error on Power System Imbalances and Operating Reserve Requirements

Four simulations are performed for this scenario. The first scenario studies the impact of the SCUC baseline error on the power system imbalances, while the other three study the impact of the SCUC baseline error on three types of operating reserve requirements, namely load following, ramping and regulation. First, in order to obtain the actual unmitigated imbalances of the system, the amounts of available operating reserves are set to zero for the first simulation. Figure 5 shows the change of the power system imbalances as the SCUC baseline error increases. Each of the three graphs corresponds to a different SCED baseline error: 0, 0.05 and 0.1. It is important to mention that in the absence of the baseline error the industrial DSM is equivalent to the social welfare model. According to Figure 5, the graphs match for the whole range of the SCUC baseline error, which implies that changing the SCED baseline error has no impact on the power system imbalances. This seemingly counterintuitive outcome is explained by the fact that in the absence of load following reserves, the real-time dispatch has no flexibility to follow the

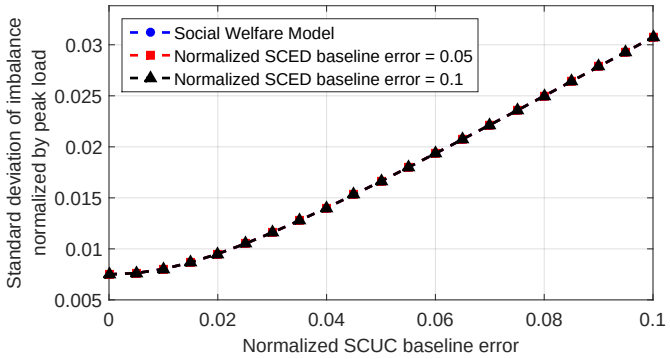

Fig. 5. Impact of SCUC baseline error on power system imbalances

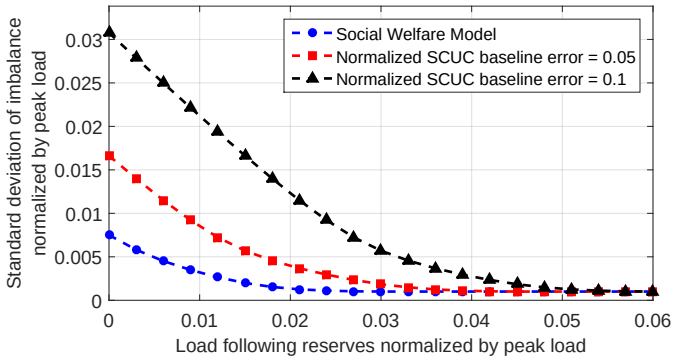

Fig. 6. Impact of SCUC baseline error on load following reserve requirement

erroneous setpoints affected by the SCED baseline error. On the other hand, the results show that increasing the SCUC baseline error to 10% increases the imbalances four times. This indicates that the SCUC baseline error is likely to have significant impact on the reserve requirements.

Next, the impact of the SCUC baseline error on each type of reserve requirements is studied. Figures 6 and 7 show the load following and ramping reserve requirements for three values of the SCUC baseline error: 0, 0.05 and 0.1. The curves in Figure 6 reach saturation for different values of load following reserves, which shows that the system with higher SCUC baseline error have higher load following reserve requirement. In contrast, Figure 7 shows that the ramping reserve requirement is affected by the day-ahead forecast error only slightly. The differences are only noticeable for small values of the ramping reserve requirement, and the graphs merge before reaching

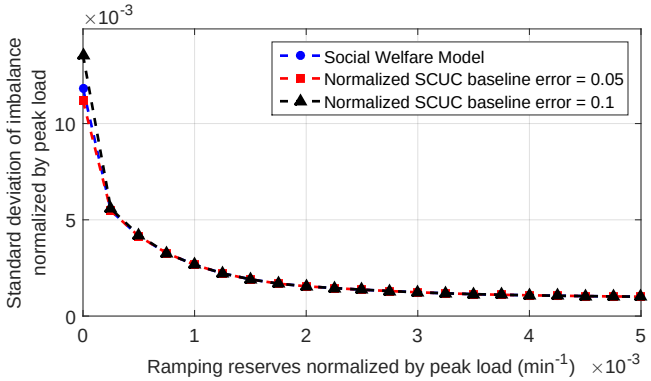

Fig. 7. Impact of SCUC baseline error on ramping reserve requirement

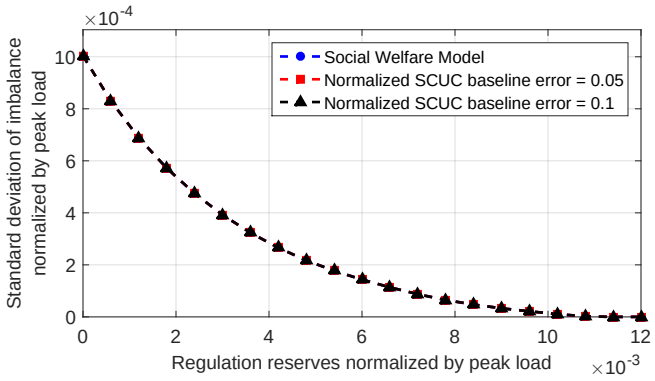

Fig. 8. Impact of SCUC baseline error on regulation reserve requirement

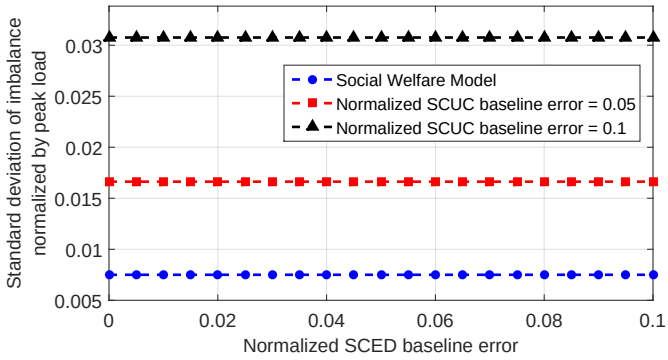

Fig. 9. Impact of SCED baseline error on power system imbalance

the saturation. This is because the SCUC baseline error appears in the ramping reserve scheduling process in a differential form. The ramping reserve requirement is more sensitive towards high variability [72]–[75]. Also, for both figures, all three graphs have the same saturation level, which means that the effect of the SCUC baseline error is completely mitigated at this timescale and is prevented from mitigating to smaller timescales. This phenomenon is clearly demonstrated in Figure 8, where all three graphs replicate each other identically. As expected, the regulation reserve requirement is the same for all three values of the SCUC baseline error.

C. Impact of SCED Baseline Error on Power System Imbalances and Operating Reserve Requirements

Four simulations are performed for this scenario. The first scenario studies the impact of the SCED baseline error on the power system imbalances, while the other three study the impact of the SCED baseline error on three types of operating reserve requirements, namely load following, ramping and regulation. Figure 9 shows the change of the power system imbalances as the SCED baseline error increases. Each of the three graphs corresponds to a different SCUC baseline error: 0, 0.05 and 0.1. According to Figure 5, the graphs remain unchanged for the whole range of the SCED baseline error, which agrees with the results in the previous scenario that changing the SCED baseline error has no impact on the power system imbalances. This, again, is explained by the absence of load following reserves.

Next, the impact of the SCED baseline error on each type of reserve requirements is studied. Figure 10 and 11 show the load following and ramping reserve requirements for three values of the SCED baseline error: 0, 0.05 and 0.1. The resulting curves look counter-intuitive but can be easily explained. Similar outcomes are observed when studying the impact of the short-term forecast error on load following and ramping reserve requirements [53], [54]. The conventional wisdom is that adding load following and ramping reserves *always* improves power system imbalances. However, this is not always true. In the absence of load following or ramping reserves, the system has no flexibility and the generation units follow the schedule defined in the day-ahead market. However, as the load

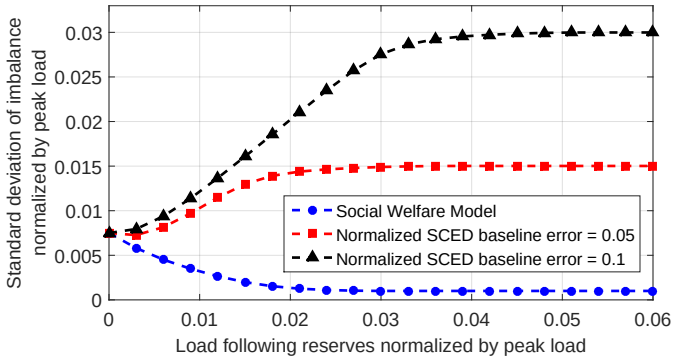

Fig. 10. Impact of SCED baseline error on load following reserve requirement

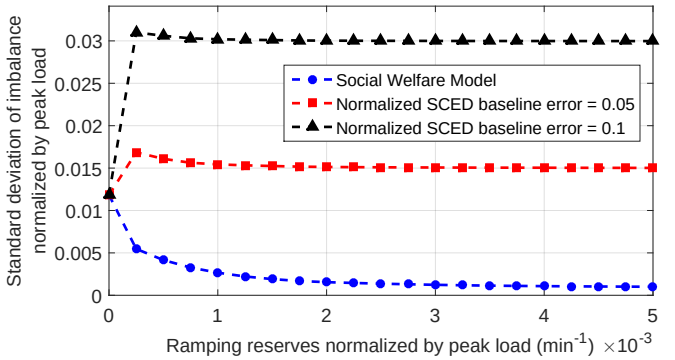

Fig. 11. Impact of SCED baseline error on ramping reserve requirement

following and ramping reserves are added to the system, the generation units' added flexibility wrongly track the erroneous net load affected by the SCED baseline error. Such a scenario, however, is purely theoretical.

Since neither load following nor ramping reserves are able to mitigate the imbalances in the case of the SCED baseline error, the regulation reserves are the only solution. Since the SCED baseline error creates imbalances when the generators ramp from the current level to the new dispatched value, it is expected that increasing amount of regulation reserves should mitigate the imbalances in this scenario. Figure 12 shows the impact of increasing the regulation reserves on the imbalances of the power system for three different values of the SCED baseline error. The curves show that higher SCED baseline error leads to higher regulation reserve requirement.

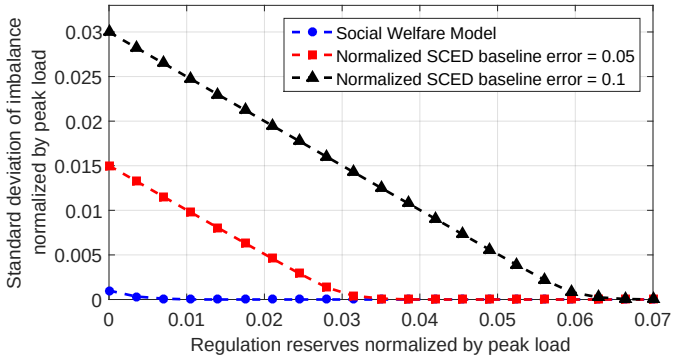

Fig. 12. Impact of SCED baseline error on regulation reserve requirement

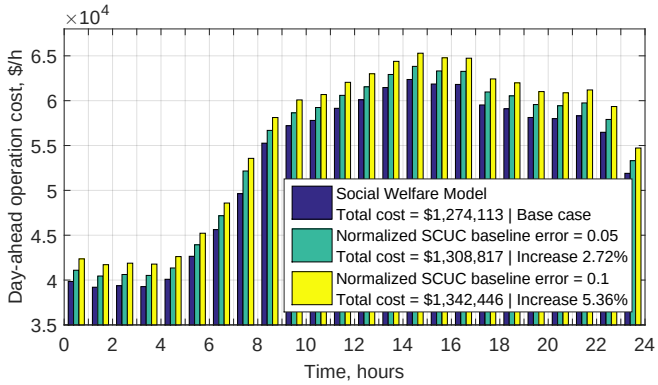

Fig. 13. Impact of SCUC baseline error on day-ahead operation cost

D. Impact of SCUC Baseline Error on Power System Operation Cost and Electricity Market Price

This subsection studies the impact of the SCUC baseline error on the power system operation cost and the electricity market price. Three different values of the SCUC baseline error are considered: 0, 0.05 and 0.1, while the SCED baseline error is assumed to be zero for this scenario. The impact on both day-ahead and real-time operations is studied. It is important to notice that since the SCUC baseline error occurs during the day-ahead scheduling operations, its impact on the day-ahead operations is certain expected. In contrast, the real-time operations belong to a faster timescale. As a result, for the impact of the SCUC baseline error on the real-time operations to exist, there should be a coupling between the respective timescales. This is where the enterprise control has to play its role. Integration of the control layers operating at different timescales allows the detection of coupling between these timescales.

First, the impact on the day-ahead operation is studied. Figure 13 shows that the SCUC baseline inflation leads to increased day-ahead scheduling cost. This is an obvious outcome and is explained by the fact that the SCUC baseline inflation is equivalent to having higher net load and, therefore, more scheduled generation. Besides the SCUC baseline error, the cost increase magnitude depends on the power system generation base. If the system had to commit an additional expensive unit to accommodate the inflated baseline, the cost difference would be noticeably higher. Similarly, Figure 14 shows how the day-ahead market price changes in the presence of the SCUC baseline error. The price curves in Figure 14 have trends similar to the cost curves in Figure 13; higher price corresponds to higher net load. However, there are few important differences that provide an insight into the market price formation. First, the market price sharply increases around the 7-th or 8-th hour, in contrast to the smoothly increasing cost in Figure 13. This is explained by the fact that the electricity market price is defined by the marginal generation units that are usually more expensive than the base generators. Second, in the presence of the baseline error, the market price drops when moving from 7-th to 8-th hour, while the net load increases during the same period. This seemingly counterintuitive result has a simple explanation. Since the generators have quadratic cost functions, the higher output they have, the more expensive an additional MW of generation becomes (the market price). Thus, since commitment of an additional generator reduces the partial load on each unit, it also reduces the market price. On the other hand, commitment of an additional generator comes with a fixed startup and operation costs. This is what Figure 14 demonstrates; during the 8-th hour a new generator is committed which reduces the market price, but also increases the operation cost due to added fixed costs as shown in Figure 14. The third point is related to the previous one. The market price during the 8-th hour is the lowest when the baseline error is equal to 0.05. As stated above, the presence of the baseline error is equivalent to higher net load. As a result, commitment of an additional generator during the 8-th hour becomes more economical, reducing the market price. In contrast, since the effective net load is lower in the absence of the baseline error, the additional fixed costs make committing an additional generator uneconomical.

Next, the impact of the SCUC baseline error on the real-time operations is studied. Figure 15 shows that the real-time operation costs match for the most part of the simulation period. As discussed at the beginning of this subsection, this is due to the different timescales of the SCUC baseline error and the real-time operation. However, there is a noticeable difference during the 8-th hour; the operation cost is slightly higher in the presence of the

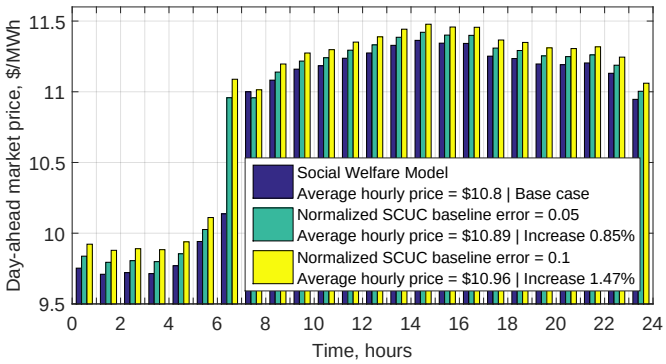

Fig. 14. Impact of SCUC baseline error on electricity day-ahead market price

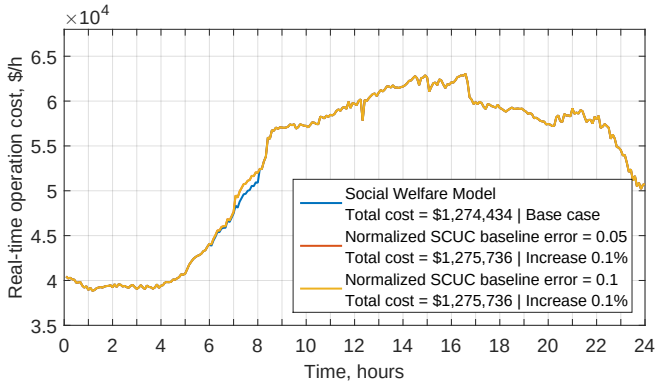

Fig. 15. Impact of SCUC baseline error on real-time operation cost

SCUC baseline error. This cost difference corresponds to the fixed cost of the additional generator committed for that hour, as discussed above. Since there is no SCED baseline error, the real-time net loads are identical for the three cases and, therefore, identical dispatches are obtained for the rest of the simulation period. The real-time market prices are also nearly identical as shown in Figure 16. The difference is that, during the 8-th hour, the market price is lower in the presence of the baseline error. This is again due to the additional generator committed for that hour, which reduces the market price. The magnitude of this phenomenon depends on the generation base of the system as well as the net load profile. It is possible to observe such decrease of the real-time market price at multiple hours during the day. Thus, it can be concluded that the presence of the SCUC baseline error increases the day-ahead operation cost and market price. Its impact also propagates down the enterprise control control layers to

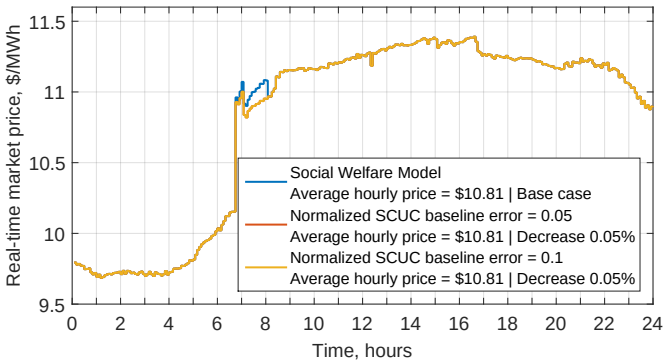

Fig. 16. Impact of SCUC baseline error on electricity real-time market price

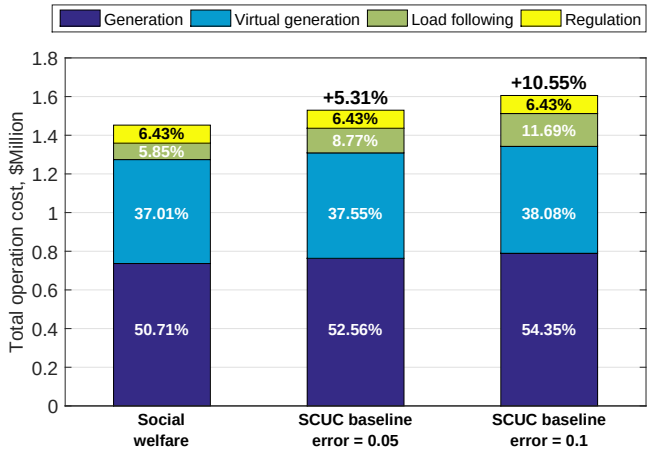

Fig. 17. Cost breakdown for social welfare and industrial DSM models

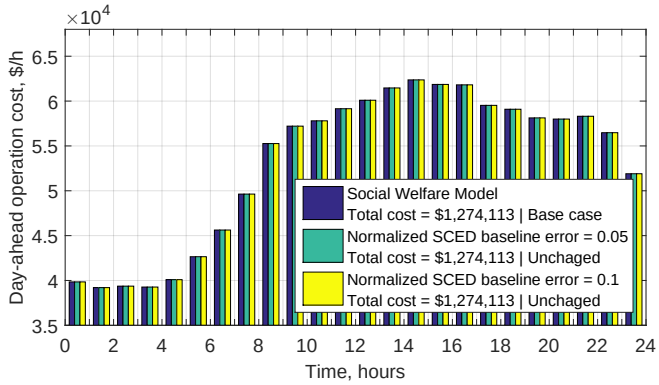

Fig. 18. Impact of SCED baseline error on day-ahead operation cost

the real-time operations.

In addition to the operation costs discussed here, the presence of the SCUC baseline error also increases the load following reserve requirement as demonstrated above. This further increases the total operation cost of the system. The comparison of cost breakdowns for social welfare and industrial DSM models is presented in Figure 17. The percentage of each section shows what portion of the social welfare model total cost it equals. The results show that the total cost increases by 10.55% when the SCUC baseline error reaches 10%. In contrast, the operation cost associated with only generation dispatch and DSM compensations increases by 5.36% as shown in Figure 13. This difference corresponds to the cost of additional load following reserves.

E. Impact of SCED Baseline Error on Power System Operation Cost and Electricity Market Price

This subsection studies the impact of the SCED baseline error on the power system operation cost and the electricity market price. Three different values of the SCED baseline error are considered: 0, 0.05 and 0.1, while the SCUC baseline error is assumed to be zero for this scenario. The impact on both day-ahead and real-time operations is studied. It is important to notice that since the SCED baseline error occurs during the real-time balancing operations, its impact on the real-time operations is certain expected. In contrast, the day-ahead operations belong to a slower timescale. As a result, for the impact of the SCED baseline error on the day-ahead operations to exist, there should be a coupling between the respective timescales.

First, the impact on the day-ahead operation is studied. Figure 18 the day-ahead scheduling costs are identical for the three SCED baseline errors. Similarly, the SCED baseline error has no impact on the day-ahead market price as shown in Figure 19. This is explained by the fact that the day-ahead scheduling happens in advance, before the

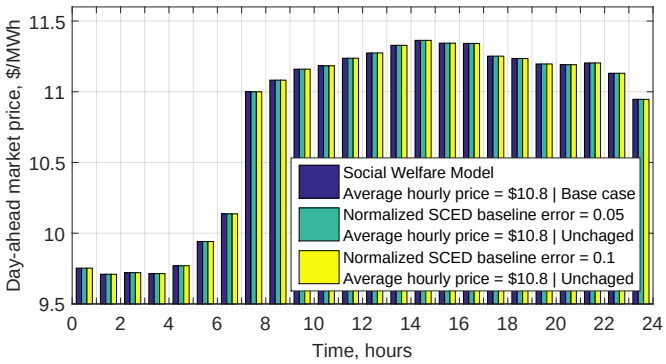

Fig. 19. Impact of SCED baseline error on electricity day-ahead market price

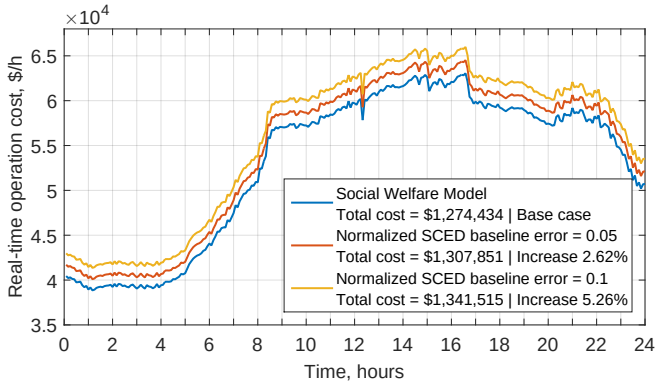

Fig. 20. Impact of SCED baseline error on real-time operation cost

real-time operations start. Therefore, the SCED baseline error, occurring during the real-time operations, is unable to affect the day-ahead operations.

Next, the impact on the real-time operations is studied. As shown in Figure 20, higher SCED baseline error leads to higher real-time operation cost due to the additionally dispatched generation to meet the inflated baseline. Similarly, Figure 21 shows that inflation of the SCED baseline also increases the real-time market price. Similar to one of the cases studied above, the market price in Figure 21 drops when moving from 7-th to 8-th hour, while the net load increases during the same period. This is again due to commitment of an additional generator in SCUC during the 8-th hour. The major difference in this case is that the SCUC baseline error is zero. Thus, all three curves in Figure 21 have the set of committed generators. As a result, all three experience the same price drop during the 8-th hour. The difference in their actual values is due to the SCED baseline error.

Similar to the case with SCUC baseline error, the presence of the SCED baseline error also increases the regulation reserve requirement as demonstrated above. This further increases the total operation cost of the system. The comparison of cost breakdowns for social welfare and industrial DSM models is presented in Figure 22. The results show that the total cost increases by 35.69% when the SCED baseline error reaches 10%. The major part of that increase is due to procurement of additional regulation reserves. It should be noted, that the results in Figure 6 and Figure 12 show comparable increase of the load following and regulation reserve requirements in the presence of SCUC and SCED baseline errors respectively. However, higher cost of the operating reserves results in more significant increase of the total cost as shown in Figure 22.

VI. Recommendations

Previous sections have shown that the presence of a baseline error in the industrial DSM formulation increases the power system operating reserve requirements, the overall operating costs and imposes potential reliability risks. This is likely to be of concern to ISOs and RTOs. As the baseline error increases, more energy is wasted in both the day-ahead and real-time operations to meet a counter-factual demand. Furthermore, procurement of more operating

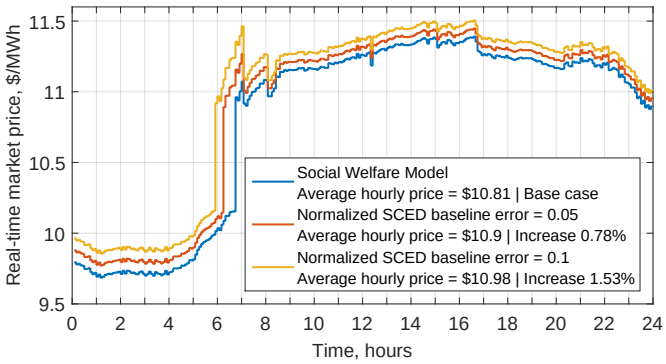

Fig. 21. Impact of SCED baseline error on electricity real-time market price

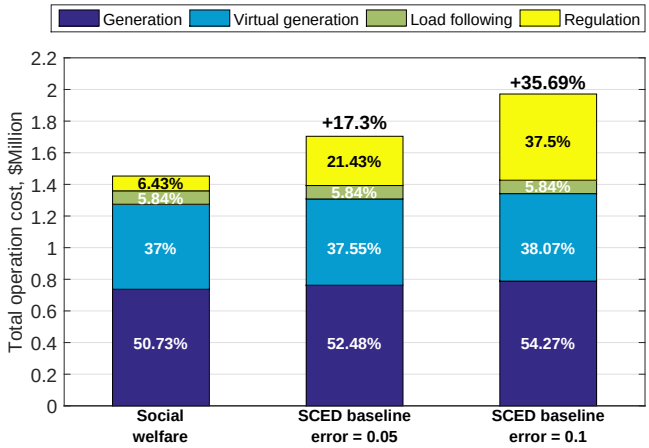

Fig. 22. Cost breakdown for social welfare and industrial DSM models

reserves is required to achieve the same levels of reliability. Based on these results, potential baseline inflation should be given attention by policy-makers (e.g. FERC). The effects of industrial baseline errors can be mitigated with effective policy. As a first solution, the industrial baseline can be calculated using the same methods as the short-term stochastic load prediction. Such an approach leaves less potential for baseline manipulation. A more comprehensive solution to this problem will be the upcoming trend of transactive energy [89]–[92] which is consonant with the social welfare method and would eliminate the concept of baseline and the associated uncertainties.

VII. Conclusion

This paper compares the social welfare and industrial DSM implementations using the power system enterprise control model. The presence of the baseline in the industrial model introduces one more forecastable parameter with related uncertainties. This paper uses a multi-layer enterprise control simulator with DSM models incorporated into the day-ahead and the real-time market structures. The simulation results show that the baseline errors in the industrial model result in erroneously high dispatch levels in both the day-ahead and real-time markets and increase the potential imbalances of the system. Increased dispatch levels lead to increased overall operation costs and electricity market prices. On the other hand, increased levels of imbalances require increased amounts of power system operating reserves, adding to the overall costs. The social welfare model or a revised baseline forecast method should be adopted by the ISOs to save energy and reduce costs.

References

[1] B. Jiang, A. M. Farid, K. Youcef-Toumi, Demand Side Management in A Day-Ahead Wholesale Market: A Comparison of Industrial & Social Welfare Approaches, Applied Energy 1 (2015) 642–654.

[2] P. Palensky, D. Dietrich, Demand Side Management: Demand Response, Intelligent Energy Systems, and Smart Loads, IEEE Transactions on Industrial Informatics 7 (3) (2011) 381–388.

[3] R. Dhulst, W. Labeeuw, B. Beusen, S. Claessens, G. Deconinck, K. Vanthournout, Demand response flexibility and flexibility potential of residential smart appliances: Experiences from large pilot test in Belgium, Applied Energy 155 (2015) 79 – 90. doi:http://dx.doi.org/10.1016/j.apenergy.2015.05.101.
URL http://www.sciencedirect.com/science/article/pii/S0306261915007345

[4] L. Chen, N. Li, L. Jiang, S. H. Low, Optimal Demand Response: Problem Formulation and Deterministic Case, Control and Optimization Methods for Electric Smart Grids 3 (2012) 63–85.

[5] G. Strbac, Demand side management: Benefits and challenges, Energy Policy 36 (12) (2008) 4419–4426.

[6] H. Wolisz, C. Punkenburg, R. Streblow, D. Mller, Feasibility and potential of thermal demand side management in residential buildings considering different developments in the german energy market, Energy Conversion and Management 107 (2016) 86 – 95, special Issue on Efficiency, Cost, Optimisation, Simulation and Environmental Impact of Energy Systems (ECOS)-2014. doi:http://dx.doi.org/10.1016/j.enconman.2015.06.059.
URL http://www.sciencedirect.com/science/article/pii/S0196890415006007

[7] M. Y. Ramandi, K. Afshar, A. S. Gazafroudi, N. Bigdeli, Reliability and economic evaluation of demand side management programming in wind integrated power systems, International Journal of Electrical Power & Energy Systems 78 (2016) 258 – 268. doi:http://dx.doi.org/10.1016/j.ijepes.2015.11.075.
URL http://www.sciencedirect.com/science/article/pii/S0142061515005062

[8] A. Mohd Zin, M. Moradi, A. Khairuddin, M. Moradi, An analytical literature review of the available techniques for relieving transmission line bottleneck in deregulated power systems, Applied Mechanics and Materials 124-128 (2016) 818.

[9] D. Patteeuw, G. Reynders, K. Bruninx, C. Protopapadaki, E. Delarue, W. Dhaeseleer, D. Saelens, L. Helsen, abatement cost of residential heat pumps with active demand response: demand- and supply-side effects, Applied Energy 156 (2015) 490 – 501. doi:http://dx.doi.org/10.1016/j.apenergy.2015.07.038.
URL http://www.sciencedirect.com/science/article/pii/S0306261915008673

[10] G. Wang, Q. Zhang, H. Li, B. C. McLellan, S. Chen, Y. Li, Y. Tian, Study on the promotion impact of demand response on distributed {PV} penetration by using non-cooperative game theoretical analysis, Applied Energydoi:http://dx.doi.org/10.1016/j.apenergy.2016.01.016.
URL http://www.sciencedirect.com/science/article/pii/S0306261916000350

[11] A. Arteconi, E. Ciarrocchi, Q. Pan, F. Carducci, G. Comodi, F. Polonara, R. Wang, Thermal energy storage coupled with PV panels for demand side management of industrial building cooling loads, Applied Energydoi:http://dx.doi.org/10.1016/j.apenergy.2016.01.025.
URL http://www.sciencedirect.com/science/article/pii/S0306261916300058

[12] F. Sossan, V. Lakshmanan, G. T. Costanzo, M. Marinelli, P. J. Douglass, H. Bindner, Grey-box modelling of a household refrigeration unit using time series data in application to demand side management, Sustainable Energy, Grids and Networks 5 (2016) 1 – 12. doi:http://dx.doi.org/10.1016/j.segan.2015.10.003.
URL http://www.sciencedirect.com/science/article/pii/S2352467715000533

[13] R. Menke, E. Abraham, P. Parpas, I. Stoianov, Demonstrating demand response from water distribution system through pump scheduling, Applied Energy 170 (2016) 377 – 387. doi:http://dx.doi.org/10.1016/j.apenergy.2016.02.136.
URL http://www.sciencedirect.com/science/article/pii/S0306261916302926

[14] D. P. Chassin, J. Stoustrup, P. Agathoklis, N. Djilali, A new thermostat for real-time price demand response: Cost, comfort and energy impacts of discrete-time control without deadband, Applied Energy 155 (2015) 816 – 825. doi:http://dx.doi.org/10.1016/j.apenergy.2015.06.048.
URL http://www.sciencedirect.com/science/article/pii/S0306261915008065

[15] B. P. Esther, K. S. Kumar, A survey on residential demand side management architecture, approaches, optimization models and methods, Renewable and Sustainable Energy Reviews 59 (2016) 342 – 351. doi:http://dx.doi.org/10.1016/j.rser.2015.12.282.
URL http://www.sciencedirect.com/science/article/pii/S1364032115016652

[16] O. Kilkki, A. Alahivl, I. Seilonen, Optimized control of price-based demand response with electric storage space heating, IEEE Transactions on Industrial Informatics 11 (1) (2015) 281–288. doi:10.1109/TII.2014.2342032.

[17] C. Li, X. Yu, W. Yu, G. Chen, J. Wang, Efficient computation for sparse load shifting in demand side management, IEEE Transactions on Smart Grid PP (99) (2016) 1–12. doi:10.1109/TSG.2016.2521377.

[18] G. Bianchini, M. Casini, A. Vicino, D. Zarrilli, Demand-response in building heating systems: A model predictive control approach, Applied Energy 168 (2016) 159 – 170. doi:http://dx.doi.org/10.1016/j.apenergy.2016.01.088.
URL http://www.sciencedirect.com/science/article/pii/S0306261916300757

[19] H. Darvish, A. Darvishi, H. Hejazi, Integration of demand side management in security constrained energy and reserve market, in: Innovative Smart Grid Technologies Conference (ISGT), 2015 IEEE Power Energy Society, 2015, pp. 1–5. doi:10.1109/ISGT.2015.7131892.

[20] A. D. Giorgio, F. Liberati, A. Lanna, Real time optimal power flow integrating large scale storage devices and wind generation, in: Control and Automation (MED), 2015 23th Mediterranean Conference on, 2015, pp. 480–486. doi:10.1109/MED.2015.7158794.

[21] H. Yang, T. Xiong, J. Qiu, D. Qiu, Z. Y. Dong, Optimal operation of des/cchp based regional multi-energy prosumer with demand response, Applied Energy 167 (2016) 353 – 365. doi:http://dx.doi.org/10.1016/j.apenergy.2015.11.022.
URL http://www.sciencedirect.com/science/article/pii/S0306261915014634

[22] D. Setlhaolo, X. Xia, Combined residential demand side management strategies with coordination and economic analysis, International Journal of Electrical Power & Energy Systems 79 (2016) 150 – 160. doi:http://dx.doi.org/10.1016/j.ijepes.2016.01.016.
URL http://www.sciencedirect.com/science/article/pii/S014206151600017X

[23] B. Alimohammadisagvand, J. Jokisalo, S. Kilpelinen, M. Ali, K. Sirn, Cost-optimal thermal energy storage system for a residential building with heat pump heating and demand response control, Applied Energy 174 (2016) 275 – 287. doi:http://dx.doi.org/10.1016/j.apenergy.2016.04.013.
URL http://www.sciencedirect.com/science/article/pii/S0306261916304640
[24] L. Ju, Z. Tan, J. Yuan, Q. Tan, H. Li, F. Dong, A bi-level stochastic scheduling optimization model for a virtual power plant connected to a windphotovoltaicenergy storage system considering the uncertainty and demand response, Applied Energy 171 (2016) 184 – 199. doi:http://dx.doi.org/10.1016/j.apenergy.2016.03.020.
URL http://www.sciencedirect.com/science/article/pii/S0306261916303312
[25] D. Stimoniaris, T. Kollatou, D. Tsiamitros, M. Zehir, A. Batman, M. Bagriyanik, A. Ozdemir, E. Dialynas, Demand-side management by integrating bus communication technologies into smart grids, Electric Power Systems Research 136 (2016) 251 – 261. doi:http://dx.doi.org/10.1016/j.epsr.2016.02.026.
URL http://www.sciencedirect.com/science/article/pii/S0378779616300414
[26] E. Karfopoulos, L. Tena, A. Torres, P. Salas, J. G. Jorda, A. Dimeas, N. Hatziargyriou, A multi-agent system providing demand response services from residential consumers, Electric Power Systems Research 120 (2015) 163 – 176. doi:http://dx.doi.org/10.1016/j.epsr.2014.06.001.
URL http://www.sciencedirect.com/science/article/pii/S0378779614002089
[27] A. Gomez-Exposito, A. J. Conejo, C. Canizares, Electric Energy Systems: Analysis and Operation, CRC Press, 2008.
[28] C. Zhao, J. Wang, J. P. Watson, Y. Guan, Multi-stage robust unit commitment considering wind and demand response uncertainties, IEEE Transactions on Power Systems 28 (3) (2013) 2708–2717. doi:10.1109/TPWRS.2013.2244231.
[29] V. K. Tumuluru, Z. Huang, D. H. K. Tsang, Integrating price responsive demand into the unit commitment problem, IEEE Transactions on Smart Grid 5 (6) (2014) 2757–2765. doi:10.1109/TSG.2014.2331357.
[30] N. Rahbari-Asr, U. Ojha, Z. Zhang, M. Y. Chow, Incremental welfare consensus algorithm for cooperative distributed generation/demand response in smart grid, IEEE Transactions on Smart Grid 5 (6) (2014) 2836–2845. doi:10.1109/TSG.2014.2346511.
[31] E. Nekouei, T. Alpcan, D. Chattopadhyay, Game-theoretic frameworks for demand response in electricity markets, IEEE Transactions on Smart Grid 6 (2) (2015) 748–758. doi:10.1109/TSG.2014.2367494.
[32] N. iek, H. Deli, Demand response management for smart grids with wind power, IEEE Transactions on Sustainable Energy 6 (2) (2015) 625–634. doi:10.1109/TSTE.2015.2403134.
[33] K. Matsumoto, Y. Takamuki, N. Mori, M. Kitayama, An interactive approach to demand side management based on utility functions, in: International Conference on Electric Utility Deregulation and Restructuring and Power Technologies, 2000., 2000, pp. 147–150.
[34] L. Na, L. Chen, S. H. Low, Optimal demand response based on utility maximization in power networks, in: 2011 IEEE Power and Energy Society General Meeting, IEEE Power and Energy Society General Meeting, IEEE Computer Society, 2011, pp. 1–8.
[35] M. Roozbehani, M. Dahleh, S. Mitter, On the Stability of Wholesale Electricity Markets under Real-Time Pricing, in: 2010 49th IEEE Conference on Decision and Control, 2010, pp. 1911–1918.
[36] FERC, Final Rule, Order 719, Wholesale Competition in Regions with Organized Electric Markets, Tech. rep., FERC (2008).
[37] R. Walawalkar, S. Fernands, N. Thakur, K. R. Chevva, Evolution and current status of demand response (DR) in electricity markets: Insights from PJM and NYISO, Energy 35 (4) (2010) 1553 – 1560.
[38] M. H. Albadi, E. F. El-Saadany, A summary of demand response in electricity markets, Electric Power Systems Research 78 (11) (2008) 1989 – 1996.
[39] N. Ruiz, I. Cobelo, J. Oyarzabal, A Direct Load Control Model for Virtual Power Plant Management, IEEE Transactions on Power Systems 24 (2) (2009) 959–966.
[40] E. Karangelos, F. Bouffard, Towards Full Integration of Demand-Side Resources in Joint Forward Energy/Reserve Electricity Markets, IEEE Transactions on Power Systems 27 (1) (2012) 280–289.
[41] H.-p. Chao, Demand response in wholesale electricity markets: the choice of customer baseline, Journal of Regulatory Economics 39 (1) (2011) 68–88.
[42] S. Nolan, M. OMalley, Challenges and barriers to demand response deployment and evaluation, Applied Energy 152 (2015) 1 – 10. doi:http://dx.doi.org/10.1016/j.apenergy.2015.04.083.
URL http://www.sciencedirect.com/science/article/pii/S0306261915005462
[43] H. Cui, F. Li, Q. Hu, L. Bai, X. Fang, Day-ahead coordinated operation of utility-scale electricity and natural gas networks considering demand response based virtual power plants, Applied Energy 176 (2016) 183 – 195. doi:http://dx.doi.org/10.1016/j.apenergy.2016.05.007.
URL http://www.sciencedirect.com/science/article/pii/S030626191630589X
[44] S. M. Nosratabadi, R.-A. Hooshmand, E. Gholipour, Stochastic profit-based scheduling of industrial virtual power plant using the best demand response strategy, Applied Energy 164 (2016) 590 – 606. doi:http://dx.doi.org/10.1016/j.apenergy.2015.12.024.
URL http://www.sciencedirect.com/science/article/pii/S0306261915015974
[45] F. Wolak, J. Bushnell, B. Hobbs, The California ISOs Proxy Demand Resource (PDR) Proposal, Tech. rep. (2009).
[46] B. Jiang, A. Farid, K. Youcef-Toumi, A Comparison of Day-Ahead Wholesale Market: Social Welfare vs Industrial Demand Side Management, in: 2015 IEEE International Conference on Industrial Technology, 2015, pp. 1–7.
[47] B. Jiang, A. Farid, K. Youcef-Toumi, Impacts of Industrial Baseline Errors on Costs & Social Welfare in the Demand Side Management of Day-Ahead Wholesale Markets (in press), 2015 ASME Power & Energy Conference.
[48] E. Almeshaiel, H. Soltan, A Methodology for Electric Power Load Forecasting, Alexandria Engineering Journal 50 (2011) 137–144.
[49] California ISO, Demand Response User Guide, Tech. rep. (April 2016).
[50] PJM State & Member Training Dept., PJM Demand Side Response, Tech. rep. (2011).
[51] K. Coughlin, M. A. Piette, C. Goldman, S. Kiliccote, Estimating Demand Response Load Impacts: Evaluation of Baseline Load Models for Non Residential Buildings in California, Tech. rep. (January 2008).

[52] A. Muzhikyan, A. M. Farid, K. Youcef-Toumi, A Power Grid Enterprise Control Method for Energy Storage System Integration, IEEE Innovative Smart Grid Technologies Conference Europe. Istanbul, Turkey (2014) 1–6.
[53] A. Muzhikyan, A. M. Farid, K. Youcef-Toumi, An Enterprise Control Assessment Method for Variable Energy Resource Induced Power System Imbalances Part 1: Methodology, IEEE Transactions on Industrial Electronics 62 (4) (2015) 2448–2458.
[54] A. Muzhikyan, A. M. Farid, K. Youcef-Toumi, An Enterprise Control Assessment Method for Variable Energy Resource Induced Power System Imbalances Part 2: Results, IEEE Transactions on Industrial Electronics 62 (4) (2015) 2459 – 2467.
[55] A. Muzhikyan, A. M. Farid, K. Youcef-Toumi, Relative merits of load following reserves & energy storage market integration towards power system imbalances, International Journal of Electrical Power & Energy Systems 74 (2016) 222–229.
[56] K. Dykes, Integration of Wind into the Electricity System, Tech. rep., MIT, Cambridge (2010).
[57] J. Smith, M. Milligan, E. DeMeo, B. Parsons, Utility Wind Integration and Operating Impact State of the Art, IEEE Transactions on Power Systems 22 (3) (2007) 900–908.
[58] A. M. Farid, A. Muzhikyan, The Need for Holistic Assessment Methods for the Future Electricity Grid, in: GCC Power 2013 Conference & Exhibition, Abu Dhabi, UAE, 2013, pp. 1–13.
[59] A. M. Farid, B. Jiang, A. Muzhikyan, K. Youcef-Toumi, The need for holistic enterprise control assessment methods for the future electricity grid, Renewable and Sustainable Energy Reviews 56 (2016) 669 – 685. doi:http://dx.doi.org/10.1016/j.rser.2015.11.007.
URL http://www.sciencedirect.com/science/article/pii/S1364032115012599
[60] A. M. Farid, A. Muzhikyan, B. Jiang, K. Youcef-Toumi, The Need for Holistic Enterprise Control Assessment Methods for Enhanced Wind Integration, Bonn, Germany: World Wind Energy Association (2015) 1–13.
[61] K. De Vos, J. Driesen, Dynamic operating reserve strategies for wind power integration, IET Renewable Power Generation 8 (6) (2014) 598–610.
[62] Z. Zhou, A. Botterud, Dynamic Scheduling of Operating Reserves in Co-Optimized Electricity Markets With Wind Power, IEEE Trans. Power Syst. 29 (1) (2014) 160–171.
[63] A. Ahmadi-Khatir, A. J. Conejo, R. Cherkaoui, Multi-Area Unit Scheduling and Reserve Allocation Under Wind Power Uncertainty, IEEE Trans. Power Syst. 29 (4) (2014) 1701–1710.
[64] K. Bruninx, E. Delarue, A Statistical Description of the Error on Wind Power Forecasts for Probabilistic Reserve Sizing, IEEE Trans. Sustain. Energy 5 (3) (2014) 995–1002.
[65] V. Lakshmanan, M. Marinelli, J. Hu, H. W. Bindner, Provision of secondary frequency control via demand response activation on thermostatically controlled loads: Solutions and experiences from denmark, Applied Energy 173 (2016) 470 – 480. doi:http://dx.doi.org/10.1016/j.apenergy.2016.04.054.
URL http://www.sciencedirect.com/science/article/pii/S0306261916305128
[66] S. Behboodi, D. P. Chassin, C. Crawford, N. Djilali, Renewable resources portfolio optimization in the presence of demand response, Applied Energy 162 (2016) 139 – 148. doi:http://dx.doi.org/10.1016/j.apenergy.2015.10.074.
URL http://www.sciencedirect.com/science/article/pii/S030626191501301X
[67] A. Robitaille et al., Preliminary Impacts of Wind Power Integration in the Hydro-Quebec System, Wind Engineering 36 (1) (2012) 35–52.
[68] D. A. Halamay, T. K. A. Brekken, A. Simmons, S. McArthur, Reserve Requirement Impacts of Large-Scale Integration of Wind, Solar, and Ocean Wave Power Generation, IEEE Trans. Sustain. Energy 2 (3) (2011) 321–328.
[69] E. Ela et al., Evolution of operating reserve determination in wind power integration studies, in: IEEE Power and Energy Society General Meeting 2010, 2010, pp. 1–8.
[70] H. Saadat, Power System Analysis, McGraw-Hill, 1999.
[71] A. Gomez-Exposito, A. J. Conejo, C. Cañizares, Electric Energy Systems: Analysis and Operation, CRC, 2008.
[72] A. Muzhikyan, A. M. Farid, K. Youcef-Toumi, An enhanced method for the determination of load following reserves, in: 2014 American Control Conference, 2014, pp. 926–933. doi:10.1109/ACC.2014.6859254.
[73] A. Muzhikyan, A. M. Farid, K. Youcef-Toumi, An enhanced method for the determination of the regulation reserves, in: 2015 American Control Conference (ACC), 2015, pp. 1016–1022. doi:10.1109/ACC.2015.7170866.
[74] A. Muzhikyan, A. M. Farid, K. Youcef-Toumi, An enhanced method for the determination of the ramping reserves, in: 2015 American Control Conference (ACC), 2015, pp. 994–1001. doi:10.1109/ACC.2015.7170863.
[75] A. Muzhikyan, A. M. Farid, K. Youcef-Toumi, An A Priori Analytical Method for Determination of Operating Reserves Requirements, International Journal of Energy and Power Systems (accepted) 1 (1) (2016) 1–11.
[76] H. Holttinen et al, Methodologies to Determine Operating Reserves Due to Increased Wind Power, IEEE Trans. Sustain. Energy 3 (4) (2012) 713–723.
[77] T. Brennan, Demand-Side Management Programs Under Retail Electricity Competition, Discussion Papers dp-99-02, Resources For the Future (Oct 1998).
URL https://ideas.repec.org/p/rff/dpaper/dp-99-02.html
[78] PJM, PJM Markets & Operations Demand Response (2014).
URL http://www.pjm.com/markets-and-operations/demand-response.aspx
[79] R. Walawalkar, S. Blumsack, J. Apt, S. Fernands, An Economic Welfare Analysis of Demand Response in the PJM Electricity Market, Energy Policy 36 (10) (2008) 3692 – 3702.
[80] K.-S. Kim, L.-H. Jung, S.-C. Lee, U.-C. Moon, Security Constrained Economic Dispatch Using Interior Point Method, in: International Conference on Power System Technology (PowerCon) 2006, 2006, pp. 1–6. doi:10.1109/ICPST.2006.321680.
[81] S. Vargas, Luis, V. H. Quintana, A. Vannelli, A Tutorial Description of an Interior Point Method and Its Applications to Security-Constrained Economic Dispatch, IEEE Trans. Power Syst. 8 (3) (1993) 1315–1324. doi:10.1109/59.260862.
[82] C. Grigg et al., The IEEE Reliability Test System-1996, IEEE Trans. Power Syst. 14 (3) (1999) 1010–1020. doi:10.1109/59.780914.

[83] Q. Zhai, X. Guan, J. Yang, Fast unit commitment based on optimal linear approximation to nonlinear fuel cost: Error analysis and applications, Electric Power Systems Research 79 (11) (2009) 1604–1613.
[84] BPA, Wind Power Forecasting Data (2014).
URL http://www.bpa.gov/Projects/Initiatives/Wind/Pages/Wind-Power-Forecasting-Data.aspx
[85] BPA, Data for BPA Balancing Authority Total Load, Wind Gen, Wind Forecast, Hydro, Thermal, and Net Interchange, Tech. rep. (2014).
URL http://transmission.bpa.gov/business/operations/wind/
[86] National Renewable Energy Laboratory, High Wind Penetration Impact on U.S. Wind Manufacturing Capacity and Critical Resources, Tech. rep. (October 2006).
[87] U.S. Department of Energy, Energy Efficiency and Renewable Energy, Tech. rep. (July 2008).
[88] American Wind Energy Association, Wind integration and reliability, Tech. rep. (2013).
URL http://www.awea.org/Issues/Content.aspx?ItemNumber=5451
[89] S. Barrager, E. Cazalet, Transactive Energy: A Sustainable Business and Regulatory Model for Electricity, 1st Edition, Baker Street Publishing, 2014.
[90] E. G. Cazalet, Automated transactive energy (temix), in: Grid-Interop Forum, 2011.
[91] F. A. Rahimi, A. Ipakchi, Transactive energy techniques: closing the gap between wholesale and retail markets, The Electricity Journal 25 (8) (2012) 29–35.
[92] D. Hammerstrom, T. Oliver, R. Melton, R. Ambrosio, Standardization of a hierarchical transactive control system, Grid Interop 9 (2009) 2009.